

Coupled Inductor Based High Step-Up DC-DC Converter for Fuel Cell System Applications

Patil Anil Bhika

Research Scholar

prof.abpatil@gmail.com

Anupama Deshpande

Professor, Shri J J T University, Jhunjhunu, Rajasthan, India

mangala.d.2000@gmail.com

Dileep Kumar

Principal, VPM's Polytechnic, Thane, Maharashtra, India

dknayak@vpmthane.org

Abstract: Fuel cell can convert chemical energy of Hydrogen into electricity but with very low output voltage. A high step up dc-dc converter as a front end converter is essential for FC based application whether employed in a distributed generation system or grid connected operation. This paper presents a coupled inductor based high step-up dc-dc converter that can be used for fuel cell based applications. The proposed converter integrates voltage boost cell with the single switch coupled inductor based quadratic boost converter to achieve high voltage gain with low duty ratio and turns ratio with low voltage stress on the active switch. The small voltage stress on power devices facilitates fast switching devices with reduced losses. These features of the proposed converter reduce power losses, size and cost in addition to increased conversion efficiency. The proposed converter's operating principle and steady-state analysis are presented in detail. The proposed converter is simulated using PSpice simulation software to validate the converter operation, theoretical analysis and performance.

Keywords– DC-DC converter · Sustainable energy · Coupled inductor · High voltage gain · Low voltage stress

I – Introduction: Energy is a key source of economic development since it is a basic ingredient in many industrial and consumer activities. It is one of the most critical inputs for economic growth. Energy not only stimulates economic and social development, but it also enhances people's quality of life. As a result, global well-being and prosperity are closely linked to energy growth. Meeting the growing demand for energy in a safe and environmentally responsible manner is a big challenge. For almost 150 years, fossil fuels such as coal, oil, and natural gas have powered economies. As of 2019, fossil fuels accounted for 84 percent of global primary energy generation [1]. Fossil fuels are formed by carbon-rich remains of animals and plants that decomposed, compressed and heated underground millions of years ago. When fossil fuels are burned to generate energy, the carbon and other greenhouse gases that have been stored in them are released into the atmosphere. More over 8 million people die each year as a result of air pollution caused by fossil fuels, implying that the use of fossil fuels is responsible for one out of every five fatalities globally [2]. It is now critical to accelerate the use of non-fossil fuel clean energy. Hydrogen is considered as another promising alternative to fossil fuel. The energy from the Hydrogen can be extracted with the help of fuel cell (FC). FCs are electrochemical devices that may use hydrogen as a fuel and directly convert its chemical energy into electrical energy while producing only

water and heat as by products. The output voltage of the FC is usually very low, unstable and unregulated. As a result, a high step-up dc-dc converter is a must-have accessory for FC-based applications such as micro-grids, distribution generation, DC distribution systems, backup power, automotive, and aircraft applications where the voltage need is in the range of 380 to 400V DC.

The literature reports various boosting strategies and topologies for step-up dc-dc converters. In the switched capacitor (SC) technique, capacitors are charged in parallel and discharged in series to boost the voltage level [3], [4]. The complex nature of the SC converters due to large number of capacitors used to attain high gain and large current spike makes switched capacitor converters suitable only for small power applications. To enhance the output voltage level, inductors are magnetized in parallel and demagnetized in series in the switched inductor technique [5], [6]. Voltage multiplier circuits (VMCs) aid in achieving significant voltage gain by including a limited number of additional components [7]. VMCs are generally made up of a variety of diode and capacitor combinations to provide a high dc output voltage. Cascading multiple converter modules is another popular approach for improving the voltage gain of a dc-dc converter. The cascade structure may also be coupled with other voltage-boosting methods to further increase voltage gain [8], [9]. Cascaded converters have major downsides such as a high number of components, lower efficiency, and less system reliability. Voltage-boosting techniques based on coupled inductors have been developed during the last two decades to enhance step-up ratio, and currently they have become the most commonly utilized method [10], [11]. The coupled inductor-based boost converter can produce a high voltage boost ratio with two degrees of freedom, namely the turns ratio of the coupled inductor in addition to the duty ratio. A coupled inductor with a high turn-ratio, on the other hand, necessitates a big volume and low power density. Hence coupled inductor technique is integrated with other boosting techniques to build high step up converter with optimum turn's ratio and duty ratio.

This paper presents a single switch high step up dc-dc converter for FC based applications based on coupled inductor and cascading techniques to achieve desirable features of optimum duty ratio, optimum turn's ratio, high voltage gain, high efficiency, low ripple input current and low voltage stress on power devices.

II – Operating principle of the proposed converter

A – System configuration

Fig. 1 (a) shows the topology of the proposed high step up converter. This is a single switch two-stage quadratic boost converter with voltage boost cell. The conventional boost converter consisting Inductor L_1 , diodes D_1 , D_2 and capacitor C_1 forms the first stage of the proposed converter. The second stage is coupled inductor boost converter with an integrated voltage boost cell. The coupled inductor has two windings primary winding L_p and secondary winding L_s . The diode D_3 and capacitor C_2 placed around the coupled inductor form voltage boost cell. The D_O is output diode and C_O is output capacitor. The dc voltage source and output voltage are represented by V_{in} and V_O respectively.

The proposed converter's equivalent circuit is shown in Fig. 1(b), where the coupled inductor is represented as a combination of a magnetizing inductor L_m , a leakage inductance L_k , and an ideal transformer with corresponding turns ratio.

The currents through and voltages across devices are represented as follows: L_1 : i_{L1} , v_{L1} , L_m : i_{Lm} , v_{Lm} , L_k : i_{Lk} , v_{Lk} , D_1 : i_{D1} , v_{D1} , D_2 : i_{D2} , v_{D2} , D_3 : i_{D3} , v_{D3} , D_O : i_{D_O} , v_{D_O} , C_1 : i_{C1} , V_{C1} , C_2 : i_{C2} , V_{C2} , C_O : i_{C_O} , V_{C_O} , primary and secondary windings of coupled inductor as i_1 , i_2 and v_{Np} ,

v_{Ns} respectively. The drain-to-source and gate-to-source voltages of MOSFET switch are represented as V_{DS} and V_{GS} respectively.

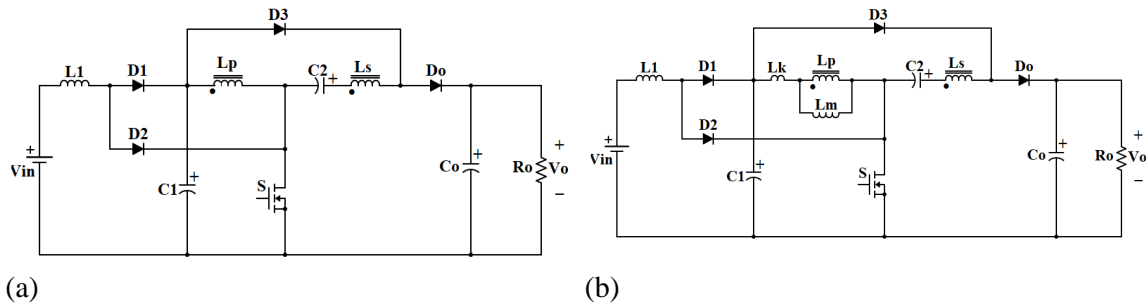


Fig. 1 (a) The proposed converter (b) Equivalent circuit

Figure 2 depicts some steady-state waveforms of the proposed converter in three operating modes in Continuous Conduction Mode (CCM) during one switching cycle.

B – Operating Principle

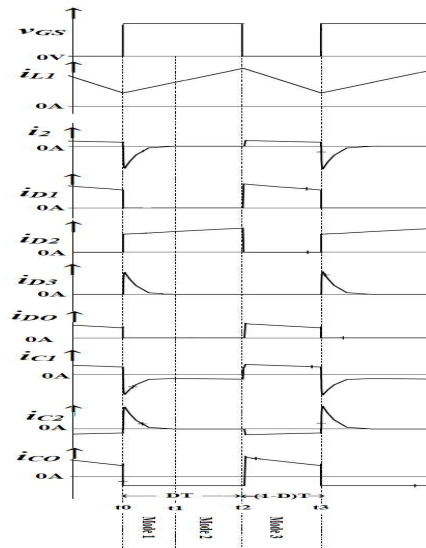
The operating principle of the proposed converter is explained on following assumptions.

- All components are ideal except the leakage inductance of coupled inductor.
- All capacitors are large enough and the voltages across them are constant.
- The inductor currents i_{L1} and i_{Lm} are continuous and always positive.
- The turns ratio of the coupled inductor n is equal to N_s/N_p .

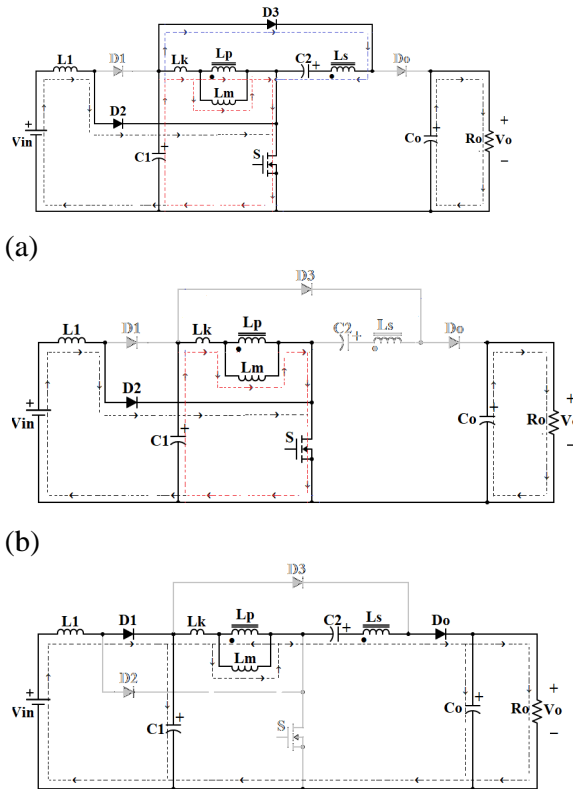
Mode 1 [t_0, t_1]: Switch S is turned on at time t_0 , which forward biases diodes D_2 and D_3 and reverse biases diodes D_1 and D_0 . Figure 3(a) depicts the current flow path. The input voltage V_{in} appears across the inductor L_1 , causing the inductor current i_{L1} to rise linearly. The voltage V_{C1} appears across the magnetising inductor L_m and leakage inductance L_k , causing i_{Lm} and i_{Lk} to rise. The energy is therefore stored in inductors L_1 , L_m , and L_k . Simultaneously, a part of the energy stored in capacitor C_1 is transferred to capacitor C_2 through diode D_3 , secondary winding, and switch S . This increases the capacitor voltage V_{C2} while decreasing the capacitor current i_{C2} linearly. At time t_1 , the decreasing capacitor current i_{C2} becomes zero, therefore turning off diode D_3 . As a result, currents i_{C2} and i_2 are forced to zero. The load current is supplied by the output capacitor C_0 . This mode will be terminated at time t_1 .

Mode 2 [t_1, t_2]: During this mode, switch S and diode D_2 stay turned ON, while diodes D_1 , D_3 , and D_0 are turned OFF. Figure 3(b) shows the current flow path. The currents i_{L1} , i_{Lm} , and i_{Lk} continue to rise in a linear fashion. During this mode, the capacitor current i_{C2} and secondary winding current i_2 are both 0. Input source V_{in} and capacitor C_1 continue to supply energy to inductors L_1 and L_m respectively. The output capacitor C_0 continues to supply the load energy. When switch S is turned OFF at time t_2 , this mode ends.

Mode 3 [t_2, t_3]: Switch S is turned OFF at time t_2 , causing diodes D_1 and D_0 to conduct while diodes D_2 and D_3 are reverse biased. Figure 3(c) depicts the current flow path. The voltage $(V_{in} - V_{C1})$ appears across the inductor L_1 . As $V_{C1} > V_{in}$, this voltage is negative. As a result, the inductor current i_{L1} decreases linearly. Capacitor C_1 receives the energy from input source V_{in} and inductor L_1 . The series voltages of the input source, inductor L_1 , primary winding,



capacitor C_2 , and secondary winding charge the output capacitor C_O and also provide the energy to the output load R_O . This mode ends at time t_3 , after which the switching cycle is repeated.



(c) **Fig. 3** Equivalent circuit and current flow diagrams for various operating modes. (a) Mode 1, (b) Mode 2, (c) Mode 3

Fig. 2 Typical wave forms

III - Steady state analysis of the proposed converter

In the simplified steady state analysis of the proposed converter the leakage inductance of coupled inductor is neglected.

Voltage gain

Following three equations can be obtained by applying KVL to Fig. 3(a)

$$V_{L1(ON)} = V_{in} \quad (1)$$

$$V_{Lm(ON)} = V_{C1} \quad (2)$$

$$V_{C2} = (1 + n)V_{C1} \quad (3)$$

Following two equations can be obtained by applying KVL to Fig. 3(c)

$$V_{L1(OFF)} = V_{in} - V_{C1} \quad (4)$$

$$V_o = V_{C1} + V_{C2} - (1 + n)V_{Lm(OFF)} \quad (5)$$

The voltage gain of the proposed converter can be determined by applying the volt-second balance principle to the inductors L_1 and L_m

$$M = \frac{V_o}{V_{in}} = \frac{2+n-D}{(1-D)^2} \quad (6)$$

Voltage stresses

The voltage stresses across the switch S, diodes D_2 and D_3 can be obtained from Fig. 3(c).

$$V_{S(OFF)} = V_{C1} - V_{Lm(OFF)} = \frac{1}{2+n-D} V_o \quad (7)$$

$$V_{D2(OFF)} = V_{Lm(OFF)} = \frac{D}{2+n-D} V_o \quad (8)$$

$$V_{D3(OFF)} = V_{C1} - V_o = \frac{1+n}{2+n-D} V_o \quad (9)$$

The voltage stresses across the diodes D_1 and D_o can be derived from Fig. 3(a).

$$V_{D1(OFF)} = V_{C1} = \frac{1-D}{2+n-D} V_o \quad (10)$$

$$V_{D0(OFF)} = V_{C1} - V_o = \frac{1+n}{2+n-D} V_o \quad (11)$$

Performance comparison with other topologies

The performance characteristics of the proposed converter and other recently published two converters [12] and [13] are compared and presented in Table I. The main parameters taken into account are components count, voltage gain and power device voltage stress. From the comparison it can be observed that the performance parameters of the proposed converter are better than the others due to use of effective voltage boost cell.

Table 1 Performance comparison with other topologies

Reference	Components# S/L/CL/D/C	Voltage gain	Voltage stress on switch	Voltage stress on output diode
[12]	1/1/1/4/3	$\frac{1+nD}{(1-D)^2}$	$\frac{V_o}{(1+nD)}$	$\frac{(2-D+nD)V_o}{(1+nD)}$
[13]	1/1/1/5/3	$\frac{1+n-D}{(1-D)^2}$	$\frac{(1+n)(1-D)V_o}{1+n-D}$	$\frac{nV_o}{1+n-D}$
Proposed converter	1/1/1/4/3	$\frac{2+n-D}{(1-D)^2}$	$\frac{V_o}{2+n-D}$	$\frac{(1+n)V_o}{2+n-D}$

#Note: S = Switch, L = Inductor, CL = Coupled Inductor, D = Diode, C = Capacitor

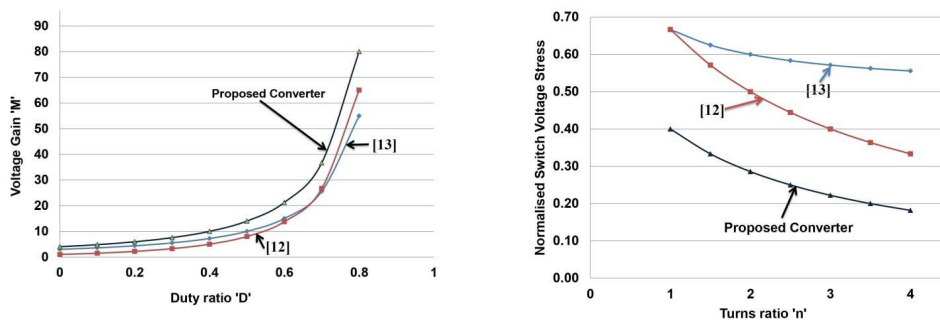
The plot of voltage gain vs duty ratio of the proposed converter and the converters reported in [12] and [13] working under the identical conditions: CCM and $n = 2$ is shown in Fig. 4(a). It

is worth noting that the proposed converter produces a larger voltage gain than other converters with the same turns ratio and duty cycle. As a result, the proposed converter can achieve the desired voltage gain with a lower turns ratio and/or duty cycle, decreasing power losses and increasing conversion efficiency.

The voltage stresses on active switches of these converters, normalized by the output voltage V_O , at duty cycle $D = 0.5$ are compared and exhibited in Fig. 4(b). The proposed converter's switch is subjected to less voltage stress than the converters reported in [12] and [13], allowing it to be built with low-voltage MOSFETs with low R_{DS_ON} , increasing efficiency while decreasing volume and cost.

IV - Results and discussion

Simulation with P Spice software is carried out to validate the working principle and the performance of the proposed converter. Figure 5 depicts the simulation circuit diagram.



(a) (b)
Fig. 4 Performance comparison with other converters (a) Voltage gain, (b) Switch voltage stress

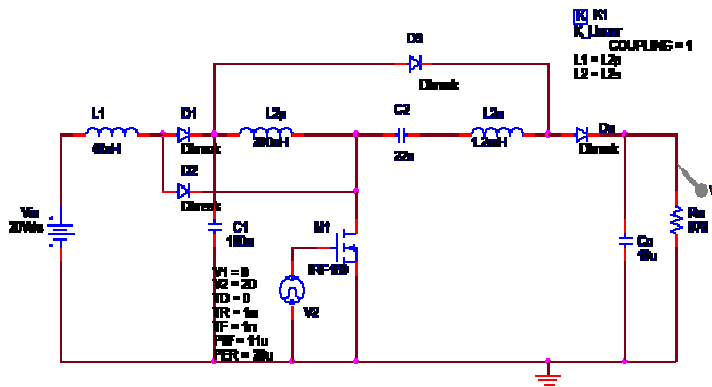


Fig. 5: PSpice simulation circuit diagram of the proposed converter

Table 2 Component values used for Simulation

Input Voltage V_{in}	20V
Output Voltage V_{out}	380V
Output Power P_o	250W
Switching frequency f_s	50 kHz
Inductor L_1	48 µH
Magnetizing inductor L_m	300 µH
Turns ratio $n = N_s/N_p$	2
Duty ratio D	0.55
Capacitor C_1	100 µF
Capacitors C_2	22 µF
Capacitors C_o	10 µF
Load resistor R_o	576Ω

The component values for the circuit are computed for a 380V output voltage, a 20V input voltage, a 250W output power, and a 50kHz switching frequency. Table 2 shows the component values chosen for simulation, as well as the duty ratio and turns ratio.

A summary of the simulation results is presented in Table 3.

Table 3 Summary of simulation result

Parameter	V_{in}	V_o	$V_{SW(OFF)}$	$V_{D0(OFF)}$	$V_{D1(OFF)}$	$V_{D2(OFF)}$	$V_{D3(OFF)}$	V_{C1}	V_{C2}
Simulation Result	20V	380V	112V	335V	41V	66V	335V	44.4V	130V

According to the simulation results, the voltage stress on active switch S is 112V, which is very modest and less than 30% of the output voltage. Because the voltage stress on the switch in the proposed converter is so minimal, it is possible to use a low voltage rated MOSFET with a low on-resistance as a switch, lowering conduction loss and cost. Because of the low voltage stresses on D_1 and D_2 , schottky diodes with a low forward voltage drop can be used to decrease diode power losses while reducing the reverse recovery problem. Although the voltage stresses on diodes D_3 and D_0 are high, they are always less than the output voltage. The right arrangement of diodes and capacitors around the coupled inductor to produce the voltage boost cell results in a high voltage gain of 19 at low turns ratio n of 2 and low duty ratio D of 0.55 with low voltage stress of 112V on the switch. The proposed converter's input current is linear and has a minimal ripple. Because the low ripple input current enhances FC stack performance, this is a significant characteristic for converters used in FC-based systems.

V – Conclusion

This paper presents a high voltage gain dc-dc converter based on coupled inductor and cascade techniques. This converter incorporates a voltage boost cell to provide significant voltage gain while maintaining a low duty ratio and turns ratio. The proper arrangement of diodes and capacitors around the coupled inductor to build the voltage boosts cell results in a high voltage gain of 19 at a turns ratio of 2 and a duty ratio of 0.55. As a result, the suggested converter achieves a very high step-up voltage gain while maintaining a low duty ratio and a low turns ratio. The voltage stress on the switch is significantly decreased and is around 30% of the output voltage. As a result, to enhance efficiency and lower the cost of the converter, a low power rated and low on-resistance MOSFET can be used as an active switch. Because an inductor is directly connected to the input voltage source in the proposed topology, the input current has a small ripple. These desired characteristics make the proposed converter an appealing alternative as front-end converter in FC applications.

References:

1. BP Statistical Review of World Energy 2020, BP, 2020, p. 4, retrieved 15 May 2021 <https://www.bp.com/content/dam/bp/business-sites/en/global/corporate/pdfs/energy-economics/statistical-review/bp-stats-review-2020-full-report.pdf>
2. Karn Vohra, Alina Vodonos, Joel Schwartz, Eloise A. Marais, Melissa P. Sulprizio, Loretta J. Mickley Global mortality from outdoor fine particle pollution generated by fossil fuel combustion: Results from GEOS-Chem, Environmental Research, Volume 195, 2021, 110754, ISSN 0013-9351, <https://doi.org/10.1016/j.envres.2021.110754>
3. Abutbul, O., Gherlitz, A., Berkovich, Y., & Ioinovici, A. [2003], "Step-up switching-mode converter with high voltage gain using a switched-capacitor circuit." IEEE Transactions on Circuits and Systems I: Fundamental Theory and Applications, 50(8), 1098–1102. ISSN: 1057-7122, doi:[10.1109/tcsi.2003.815206](https://doi.org/10.1109/tcsi.2003.815206)

4. Tang, Y., Wang, T., & He, Y. [2014], “A Switched-Capacitor-Based Active-Network Converter With High Voltage Gain”. *IEEE Transactions on Power Electronics*, 29(6), 2959–2968, ISSN: 0885-8993, doi:[10.1109/tpel.2013.2272639](https://doi.org/10.1109/tpel.2013.2272639)
5. Axelrod, B., Berkovich, Y., & Ioinovici, A. [2008]. “Switched-Capacitor/Switched-Inductor Structures for Getting Transformerless Hybrid DC–DC PWM Converters”, *IEEE Transactions on Circuits and Systems I: Regular Papers*, 55(2), 687–696, ISSN: 1549-8328, doi:[10.1109/tcsi.2008.916403](https://doi.org/10.1109/tcsi.2008.916403)
6. Tang, Y., Wang, T., & Fu, D. [2015]. “Multicell Switched-Inductor/Switched-Capacitor Combined Active-Network Converters”, *IEEE Transactions on Power Electronics*, 30(4), 2063–2072, ISSN: 0885-8993, doi:[10.1109/tpel.2014.2325052](https://doi.org/10.1109/tpel.2014.2325052)
7. Prudente, M., Pfitscher, L. L., Emmendoerfer, G., Romaneli, E. F., & Gules, R. [2008]. Voltage Multiplier Cells Applied to Non-Isolated DC–DC Converters. *IEEE Transactions on Power Electronics*, 23(2), 871–887. <https://doi.org/10.1109/tpel.2007.915762>
8. Ortiz-Lopez, M.G.; Leyva-Ramos, J.; Carbajal-Gutierrez, E.E.; Morales-Saldaña, J.A., [2008], “Modelling and analysis of switch-mode cascade converters with a single active switch”, *IET Power Electronics*, 2008, 1, (4), p. 478-487, ISSN 1755-4535, doi:[10.1049/iet-pel_20070379](https://doi.org/10.1049/iet-pel_20070379)
9. Leyva-Ramos, J.; Ortiz-Lopez, M.G.; Diaz-Saldierna, L.H.; Morales-Saldaña, J.A., [2009] “Switching regulator using a quadratic boost converter for wide DC conversion ratios”, *IET Power Electronics*, 2009, 2, (5), p. 605-613, doi:[10.1049/iet-pel.2008.0169](https://doi.org/10.1049/iet-pel.2008.0169)
10. G. Wu, X. Ruan and Z. Ye, [2018], “High Step-Up DC–DC Converter Based on Switched Capacitor and Coupled Inductor”, *IEEE Transactions on Industrial Electronics*, vol. 65, no. 7, pp. 5572-5579, July 2018, ISSN 1755-4535, doi: 10.1109/TIE.2017.2774773.
11. Zhao, Y.; Li, W.; Deng, Y.; He, X., [2011], “High step-up boost converter with passive lossless clamp circuit for non-isolated high step-up applications”, *IET Power Electronics*, 2011, 4, (8), p. 851-859, ISSN 1755-4535, doi:[10.1049/iet-pel.2010.0232](https://doi.org/10.1049/iet-pel.2010.0232)
12. [Jahangiri, H., Mohammadpour, S., & Ajami, A. \(2018, February\). A high step-up DC-DC boost converter with coupled inductor based on quadratic converters. 2018 9th Annual Power Electronics, Drives Systems and Technologies Conference \(PEDSTC\), 20–25. https://doi.org/10.1109/pedstc.2018.8343765](https://doi.org/10.1109/pedstc.2018.8343765)
13. [Lee, S. W., & Do, H. L. \(2019\). Quadratic Boost DC–DC Converter With High Voltage Gain and Reduced Voltage Stresses. IEEE Transactions on Power Electronics, 34\(3\), 2397–2404. https://doi.org/10.1109/tpel.2018.2842051](https://doi.org/10.1109/tpel.2018.2842051)